Journal Pre-proof

Loss of GLP-2R signaling in *Glp2r*$^{-/-}$ mice increases the long-term severity of graft versus host disease

Bernardo Yusta, Chi Kin Wong, Dianne Matthews, Jacqueline A. Koehler, Laurie L. Baggio, Daniel J. Drucker

PII: S2212-8778(25)00218-2

DOI: https://doi.org/10.1016/j.molmet.2025.102311

Reference: MOLMET 102311

To appear in: *Molecular Metabolism*

Received Date: 21 November 2025

Revised Date: 11 December 2025

Accepted Date: 12 December 2025

Please cite this article as: Yusta B, Wong CK, Matthews D, Koehler JA, Baggio LL, Drucker DJ, Loss of GLP-2R signaling in *Glp2r*$^{-/-}$ mice increases the long-term severity of graft versus host disease, *Molecular Metabolism*, https://doi.org/10.1016/j.molmet.2025.102311.

Loss of GLP-2R signaling in *Glp2r*$^{-/-}$ mice increases the long-term severity of graft versus host disease

Bernardo Yusta, Chi Kin Wong, Dianne Matthews, Jacqueline A Koehler, Laurie L Baggio and Daniel J Drucker

From the Lunenfeld Tanenbaum Research Institute, Mt. Sinai Hospital, Toronto Ontario Canada M5G1X7

Address correspondence to:

Dr. Daniel J Drucker
Mt. Sinai Hospital, LTRI
600 University Avenue Mailbox39
Toronto ON M5G 1X7
V 416-361-2661 drucker@lunenfeld.ca

Competing interests: D.J.D. has received consulting fees from Amgen, AstraZeneca Inc, Alnylam, Crinetics Eli Lilly Inc, Insulet, Kallyope, Metsera and Pfizer Inc. and speaking fees from Novo Nordisk Inc. Mt. Sinai Hospital has received investigator-initiated grant support from Amgen, Eli Lilly Inc, Novo Nordisk, Pfizer, and Zealand Pharmaceuticals Inc to support preclinical studies in the Drucker lab.

Key words: intestine, enteroendocrine, GLP-2, barrier function, GLP-2 receptor, bacteremia,

Abstract

Background: Glucagon-like peptide-2 (GLP-2 reduces systemic and gut inflammation while preserving mucosal integrity. Preclinical and clinical reports implicate GLP-2 receptor (GLP-2R) agonism as a potential therapy for graft vs. host disease (GvHD)

Methods: Here we assessed whether enhanced vs. loss of GLP-2R signaling modifies gut injury and inflammation in experimental murine acute GvHD (aGvHD). Allogeneic hematopoietic cell transplantation (HCT) was performed using bone marrow and splenocytes from BALB/cJ donor mice to induce aGvHD in C57BL/6J recipients. Chimerism was determined by flow cytometry of immune cell compartments. Inflammation was assessed by measuring circulating cytokines and histological scoring of gut mucosal damage. GLP-2 responsivity was assessed using histology and gene expression analyses. The gut microbiome was assessed by 16S rRNA sequencing.

Results: Allogeneic chimerism was > 90% in peripheral blood and in the gut epithelial compartment. Gut GLP-2R signaling was preserved following allogeneic bone marrow transplantation. Surprisingly, GLP-2R agonism using teduglutide did not reduce circulating cytokines, gut injury, immune cell infiltration or the severity of aGvHD. In contrast, transplant recipient *Glp2r*$^{-/-}$ mice exhibited reduced survival, associated with increased bacteremia. Shifts in microbial species abundance with gain or loss of GLP-2R signaling were not correlated with aGvHD clinical outcomes.

Conclusions: Activation of GLP-2R signaling did not reduce the severity of experimental aGvHD, failing to replicate a previous study using an identical aGvHD protocol. Nevertheless, loss of GLP-2R signaling in transplant recipients decreased survival and increased bacteremia, implicating an essential role for endogenous GLP-2R signaling in maintaining barrier function in the context of immune-mediated gut epithelial injury.

1.Introduction

The enteroendocrine system is comprised of dozens of different cell types that secrete neurotransmitters and peptide hormones contributing to the control of appetite, gut motility, nutrient digestion and absorption, as well as the subsequent assimilation of amino acids, fats, and carbohydrates. Among the most extensively characterized enteroendocrine cells, the L cell secretes multiple proglucagon-derived peptides, including glucagon-like peptide-1 (GLP-1) and glucagon-like peptide-2 (GLP-2)[1]. The actions of these peptides are highly conserved across species and are mediated by structurally related yet distinct G protein coupled receptors[2]. Activation of GLP-1 receptor (GLP-1R) signaling improves glucose homeostasis and reduces appetite leading to weight loss, actions that support the approval of multiple GLP-1 medicines for the treatment of type 2 diabetes and obesity[3-5]. The GLP-2 receptor (GLP-2R) is important for control of nutrient and fluid absorption, gut motility, enterocyte mass and barrier function actions supporting development of a GLP-2R agonist, teduglutide, for the treatment of intestinal failure[2; 6].

Beyond their well-established metabolic actions, both GLP-1 and GLP-2 act locally on the gut to preserve epithelial integrity, augment barrier function[7; 8], and reduce inflammation[9]. Conversely, disruption of the gut barrier leads to augmentation of both GLP-1 and GLP-2 secretion due to L cell exposure to microbial-derived products such as lipopolysaccharide[10]. Within the gut, the GLP-1R is abundantly expressed on mucous-secreting Brunners glands, and GLP-1 medicines increase the expression of genes important for mucous production and barrier function[8]. GLP-1 also exerts cytoprotective and anti-inflammatory actions in experimental models of intestinal injury[11-14], while complete loss of GLP-1R signaling increases the extent of gut mucosal inflammation and epithelial injury in mice with dextran sulfate colitis [15]. Indeed, the anti-inflammatory and cytoprotective actions of GLP-1 underlie the hypothesis that semaglutide may be effective in reducing gut injury in patients with lymphoma undergoing high-dose chemotherapy followed by autologous haematopoietic stem cell transplantation[16].

GLP-2 also exerts multiple actions to preserve and restore mucosal health in the context of experimental intestinal injury[6]. These include enhancement of barrier function[17-19], stimulation of crypt cell proliferation and inhibition of apoptosis [20-22] and attenuation of inflammation[21; 23; 24]. These actions are evident in a wide range of preclinical models of gut inflammation and injury, and human studies illustrate the potential efficacy of the GLP-2 analogue teduglutide in children with malnutrition-associated enteropathy[25] and in adult patients with Crohn's disease [26].

More recent preclinical and clinical studies have interrogated whether the cytoprotective and anti-inflammatory actions identified for GLP-2 in the gut might be useful in the context of immune-mediated intestinal injury arising secondary to graft vs. host disease (GvHD). Studies by Norona and colleagues demonstrated that teduglutide improved GvHD outcomes and survival, and reduced intestinal mucosal damage in mice by protecting the integrity of gut intestinal stem cells (ISCs) and Paneth cells[27]. Clinical reports of 3 pediatric patients with refractory GvHD reveal substantial therapeutic responses to teduglutide administration [28]. Similarly, a retrospective survey revealed therapeutic responses to teduglutide therapy in >60% of patients with GvHD secondary to allogeneic hematopoietic cell transplantation (HCT) [29].

Accordingly, to identify potential mechanisms linking GLP-2R signaling to the modification of experimental GvHD outcomes, we evaluated the therapeutic actions of a clinically approved GLP-2R agonist in mice with gut injury secondary to acute GvHD (aGvHD) after allogeneic HCT, following the protocol used by Norona and colleagues[27]. Unexpectedly, teduglutide treatment did not result in improved survival or reduced gut injury, failing to reproduce key results of previously published studies[27]. In contrast, loss of GLP-2 receptor signaling in *Glp2r*$^{-/-}$ mice was associated with impaired survival and increased bacterial translocation across the gut mucosal barrier.

2. Material and Methods

2.1 Mice

BALB/cJ (H-2^d), B6.SJL-*Ptprc*^{a} *Pepc*^{b}/BoyJ (abbreviated to Pep Boy) and B6.129P2-*Lgr5*$^{tm1(cre/ERT2)Cle}$/J (abbreviated to Lgr5-EGFP$^+$) mice were from The Jackson Laboratory. Whole-body *Glp2r*$^{-/-}$ (GLP-2R KO) mice[30] and *Glp2r*$^{+/+}$ (WT) control mice were generated by crossing *Glp2r*$^{+/-}$ mice on the C57BL/6J genetic background in our specific pathogen-free colony at the Toronto Centre for Phenogenomics (Mt. Sinai Hospital, Toronto, ON, Canada). All experiments were performed in mice housed up to five per cage, maintained on a 12-h light/dark cycle with free access to standard rodent chow (18% kcal from fat) (Teklad global) and acidified drinking water. All experiments were conducted according to protocols approved by the Animal Care and Use Subcommittee at the Toronto Centre for Phenogenomics and were consistent with the Animal Research: Reporting In Vivo Experiments guidelines.

2.2 Hematopoietic cell transplantation (HCT)

Mouse bone marrow cells were isolated from femurs and tibiae, and splenocytes from the same donors were used as a source of T cells. Cell suspensions were prepared in DMEM:F12 media with penicillin/streptomycin, subjected to red blood cell (RBC) lysis, and counted using a hemocytometer. Congenic bone marrow chimeras (Fig. 1) were generated using Pep Boy males as donors and C57BL/6J females as recipients which were treated 1 week before and 2 weeks after transplantation with 100 mg/L neomycin and 10 mg/L polymyxin B sulfate in the drinking water[31]. The murine acute GvHD (aGvHD) model used in the current studies involved only Major Histocompatibility Complex (MHC)-fully mismatched transplants between male donor and recipient pairs and without the use of antibiotic treatment, mirroring the previously published study of teduglutide and aGvHD by Norona and colleagues[27]. Mice were 8-10 weeks of age at the time of transplantation. Recipient mice were lethally irradiated (both C57BL/6J and B6.129P2-*Lgr5*$^{tm1(cre/ERT2)Cle}$/J were given a total of 1,100 cGy, split into two equal doses 4 h apart) using a Gammacell 40 instrument as described [15; 32; 33] and subsequently reconstituted via tail vein injection. C57BL/6J recipients of congenic Pep Boy donors (congenic denotes B6.SJL-*Ptprc*^{a} *Pepc*^{b}/BoyJ mice carrying the CD45.1 protein marker from the SJL strain on a C57BL/6J genetic background) received 5x10^6 bone marrow cells whereas C57BL/6J and

Lgr5-EGFP^{+} recipients of allogeneic BALB/cJ donors received 5x10^{6} bone marrow cells and 10-15x10^{6} splenocytes. Transplantation with cells from syngeneic donors, which lack an alloreactive immune response, was used as a negative control. To minimize potential 'cage effects,' bedding from all mouse cages involved in the experiments was regularly mixed both before and after HCT. Mice were monitored daily and euthanized when they had lost ≥20% of their pre-transplantation body weight. The day of euthanasia was considered as the date of death for survival studies. Donor chimerism was assessed at sacrifice by flow cytometry on peripheral blood mononuclear cells (PBMC) and on the epithelial compartment and neighboring associated immune cells (ECI) isolated from the small intestine. Additional information on reagent identity and source is available in Supplementary Methods.

2.3 Teduglutide Treatment

The DPP-4-resistant GLP-2R agonist h[Gly^{2}]-GLP-2 (teduglutide) was from Chi Scientific Inc. Peptide stocks were diluted in phosphate buffered saline (PBS) without calcium or magnesium (vehicle) and administered to mice by subcutaneous injection at doses of 100 µg/kg BID or 200 µg/kg QD.

2.4 Tissue collection and processing

Following euthanasia, mice were weighed and the tibial length measured using an electronic caliper. The entire small intestine from the pyloric sphincter to the ileocecal junction was resected, cleaned of mesenteric fat and weight and length were determined. The length was measured under tension by suspending a 1 gram weight from the intestine distal end, prior to flushing with PBS to remove luminal content. The entire small bowel was then blotted to remove PBS before being weighed and divided into quarters. The first and third quarters were used to isolate the ECI. Adjacent 2-cm intestinal segments were collected from jejunum (sampling onwards from the 1/4 the small intestinal length distal to the pylorus) and ileum (sampling outwards from the ileocecal junction). Tissue samples were fixed in 10% neutral-buffered formalin at room temperature for 24 h, then processed and embedded in paraffin blocks, or snap-frozen in liquid nitrogen and stored at −80^{o}C for later RNA extraction.

2.5 Intestinal histomorphometry and immunohistochemistry

Paraffin sections (4 µm thick) were used for hematoxylin-eosin staining (H&E) (Sakura Finetek Tissue-Tek Prisma® *Plus* Automated Slide Stainer) and for immunohistochemistry (Leica Biosystems Bond-RX Fully Automated IHC Stainer) using an anti-GFP antibody (Cell Signaling Technology). Stained slides were scanned on a NanoZoomer (Hamamatsu Photonics) at 20x magnification and digital images analyzed using Aperio ImageScope 12.3 software (Leica Biosystems). For each mouse, a minimum of 20 well-oriented villi and crypts were selected from at least 4-5 different intestinal cross-sections. Jejunal villus height, crypt depth, the number of GFP^+ cells per crypt and GFP^+ cells per cross-section as well as ileal number of Paneth cells (identified by their eosinophilic granules) and apoptotic bodies per crypt were scored in a blinded manner. Representative digital histological images were acquired using a Leica DMR microscope equipped with a Leica DC300F camera and Leica Qwin V3 software.

2.6 Isolation of small intestine immune cells

After flushing the luminal contents with PBS, the first and third small intestine segments (as described above) were opened longitudinally and cut into small pieces. The tissue was then incubated in 5 mM ethylenediaminetetraacetic acid (EDTA), 1 mM dithiothreitol (DTT) and 10 mM HEPES in Hank's Balanced Salt Solution (HBSS) without calcium or magnesium at 37°C for 15 min in a shaker incubator and then subjected to multiple rounds of vortexing at full power for 30 seconds to fully strip the epithelial compartment and neighboring associated immune cells (ECI). Tissue fragments were removed by sequential filtering through a 500 µm strainer followed by a 100 µm strainer. The final suspension was centrifuged to pellet the cells, which were then resuspended in 44% Percoll in RPMI 1640 media at 22°C and centrifuged at 700 × g for 20 minutes. The pellet was washed twice in PBS containing 2 mM EDTA, 25 mM HEPES and 1% fetal bovine serum and processed for flow cytometry.

2.7 Flow cytometry

Samples were first treated with anti-mouse CD16/CD32 antibody (Fc block) prior to incubation for 20 min at 4°C with cell surface marker anti-mouse antibodies (clone information is provided in Supplementary Material and Methods), in parallel with the corresponding compensation and staining controls. The viability marker 4',6-diamidino-2-phenylindole (DAPI) was included to discriminate live cells. For identification of small intestine ECI allogeneic T cells, we used

antibodies against the following antigens: H-2^d, CD45.2, CD3, CD8a, CD69 and CD103. For analysis of PBMC from allogeneic HCT, we used H-2^d, CD45.2, CD3 and CD8a and for analysis of PBMC from congenic HCT, we used CD45.1 and CD45.2. Stained cells were analyzed on a Gallios flow cytometer from Beckman Coulter.

2.8 RNA extraction, cDNA synthesis and real-time qPCR

Total RNA was extracted from mouse tissues by the guanidinium thiocyanate method using TRI Reagent. Reverse transcription was performed in RNA samples treated with DNase I, using random hexamers and SuperScript III. The resulting cDNA was used for real-time qPCR performed on a QuantStudio 5 System from Thermo Fisher Scientific with TaqMan Fast Advanced Master Mix and TaqMan Gene Expression Assays (TaqMan primer information is provided in Supplementary Material and Methods). Relative quantification of transcript levels in whole intestine samples was performed using the comparative cycle threshold (Ct) method, with *Rpl32* or *Ppia* as endogenous normalization controls.

2.9 Plasma cytokine analysis

Plasma concentrations of TNF-α, IL-10, IL-12 p70, IL-1β, IL-6, CXCL1, IFNγ, IL-2, IL-4 and IL-5 were measured in samples of heparinized cardiac blood using the V-PLEX Proinflammatory Panel 1 Mouse Kit from Meso Scale Discovery as per the manufacturer's instructions.

2.10 Microbiology

Bacterial counts were quantified as colony-forming units by spread plating aliquots of tail blood on tryptic soy agar (TSA) plates incubated at 37^{o}C for 24 hours under aerobic conditions, followed by counting of the colonies grown on the plates.

2.11 16S rRNA-seq analysis

Microbiota profiling was performed using 16S rRNA gene sequencing, following methods previously described[34]. Fecal samples were collected from the distal colon, genomic DNA was extracted, and the V3–V4 hypervariable regions of the 16S rRNA gene were amplified. Amplicons were indexed, prepared into sequencing libraries, and sequenced on an Illumina MiSeq platform using 2 × 300 bp paired-end reads. Raw reads underwent adaptor removal and quality filtering before denoising and taxonomic assignment with the DADA2 pipeline[35] .

Subsequent processing used the phyloseq package[36], and differential abundance was tested using both DESeq2 [37] and LEfSe [38]. Predicted functional pathway profiles were inferred using PICRUSt2 [39].

2.12 Statistical analysis

Data are expressed as mean ± SD. As indicated in the Figure Legends, Student's t-tests and 1- or 2-way ordinary ANOVA followed by the appropriate post-hoc tests were used to calculate statistical significance. Survival curves were plotted using Kaplan-Meier estimates and compared using the Log-rank (Mantel-Cox) test. Statistical analyses and graph generation were performed using Prism 10 software from GraphPad.

3. Results

To explore mechanisms linking activation of GLP-2R signaling to attenuation of experimental GvHD severity in mice following allogeneic transplantation [27; 40], we investigated the efficacy of different teduglutide administration regimes in mitigating key pathological features of aGvHD. Additionally, we studied C57BL/6J GLP-2R knockout (GLP-2R KO; *Glp2r*$^{-/-}$) mice to assess whether loss of GLP-2R signaling would impact the outcome of aGvHD. We employed the same allogeneic murine model described in the studies of teduglutide action by Norona et al [27], in which MHC-fully mismatched hematopoietic cell transplantation (HCT) from BALB/cJ donors into C57BL/6J recipients induces robust T cell-mediated aGvHD. In this model, intestinal pathology typically emerges within 10 days post-transplantation[34; 41; 42].

An important consideration in the interpretation of experiments with allogeneic HCT using C57BL/6J GLP-2R KO recipient mice was whether the transplanted BALB/cJ cells, being *Glp2r*$^{+/+}$ cells, could contribute to GLP-2-mediated effects in the C57BL/6J GLP-2R KO recipient gut. It is well established that following myeloablative radiation exposure, transplanted bone marrow derived cells (BMDC) can fuse with somatic cells in parenchymal organs such as the intestine[43;

44] [45; 46]. This heterotypic cell fusion is frequently triggered by inflammation and tissue damage [47-49], both of which are prominent in allogeneic settings.

Previous studies have identified three distinct intestinal sites of GLP-2R expression: subepithelial stromal cells (telocytes), enteric neurons, and subpopulations of enteroendocrine cells [50-54]. All of these cell types are potential targets for BMDC-somatic cell fusion which, following BMDs nuclear reprograming, could conceivably restore GLP-2 responsiveness in C57BL/6J GLP-2R KO mice.

To address this possibility, we generated congenic bone marrow chimeras. C57BL/6J WT and C57BL/6J GLP-2R KO mice received myeloablative total body irradiation (TBI) followed by HCT using bone marrow from congenic *Glp2r*$^{+/+}$ Pep Boy donors. One-month post-transplantation, to allow time for potential fusion events, mice were treated with vehicle or the GLP-2R agonist teduglutide and canonical indicators of intestinal GLP-2 action were assessed. (Fig. 1A).

Chimerism exceeded 95% in both recipient groups as confirmed by peripheral blood mononuclear cel (PBMC) analysis (Fig 1B). Teduglutide treatment for 10 days significantly increased small intestine weight-to-length ratio, villus height, and crypt depth in C57BL/6J WT recipients of Pep Boy bone marrow (Fig. 1C), consistent with its known intestinotrophic effects [20; 55]. In contrast, no such changes were observed in C57BL/6J GLP-2R KO recipient mice.

Teduglutide also induces immediate early (IE) gene expression in the intestine [56]. Therefore, we examined the expression of several IE mRNA transcripts in C57BL/6J WT and C57BL/6J GLP-2R KO mice following an acute teduglutide challenge. As shown in Fig. 1D, transcripts such as *Egr1*, *Phlda1*, and the ErbB ligands *Areg* and *Ereg* were robustly induced in the jejunum of teduglutide-treated C57BL/6J WT mice, but not in C57BL/6J GLP-2R KO mice. At the molecular level, disruption of the *Glp2r* gene in *Glp2r*$^{-/-}$ mice results from internal deletion of exons 7 to 9 in the *Glp2r* coding sequence[30]. qPCR analysis confirmed expression of *Glp2r* exons 7-8 in C57BL/6J WT mouse jejunum while no signal was detected in C57BL/6J GLP-2R KO mouse samples (Fig. 1E). *Glp2r* mRNA levels were unaffected by teduglutide treatment in C57BL/6J WT mice.

Taken together, the histomorphometry and gene expression data (Fig. 1C and D) do not support a role for BMDC-intestinal cell fusion in mediating GLP-2-dependent effects in the gut following HCT. These findings reinforce the conclusion that endogenous GLP-2R signaling is required for teduglutide action and is not restored via WT donor-derived BMDC fusion in C57BL/6J GLP-2R KO recipients.

We next studied C57BL/6J WT and C57BL/6J GLP-2R KO recipient mice treated with vehicle or teduglutide for 4 days before undergoing allogeneic HCT with treatment continuing until sacrifice (experimental design shown in Fig. 2A). TBI was administered as pre-transplant conditioning, followed by HCT using bone marrow and splenocytes (as source of T cells) from WT BALB/cJ donors to induce aGvHD in the gastrointestinal (GI) tract. As controls, syngeneic transplants were also performed using C57BL/6J WT or C57BL/6J GLP-2R KO donors to generate aGvHD-negative mice.

Radiation injury led to a predictable body weight (BW) loss in syngeneic and allogeneic mice during the first 5 days after HCT (Fig. 2B). Subsequently, the syngeneic-transplanted mice started to regain BW, whereas the BW of the allogeneic-transplanted group continued to decline (grey shaded areas in Fig. 2B). When compared to syngeneic mice, both allogeneic C57BL/6J WT and C57BL/6J GLP-2R KO mice, irrespective of treatment, experienced similar degrees of BW loss (Fig. 2B middle and right panels) and marked upregulation of plasma proinflammatory cytokines (“cytokine storm”)[57; 58] (Fig. 2C), observations consistent with active aGvHD.

The GI tract is a major initial target organ of aGvHD [59; 60]. Early after transplantation allogeneic activated donor T cells migrate to the intestine and preferentially invade the crypt base region of the lamina propria[41]. To evaluate the recruitment of allogeneic BALB/cJ T cells to the gut, we stripped the epithelial compartment and neighbouring associated immune cells (ECI) and performed flow cytometry to assess allogeneic ECI chimerism and phenotypes. Allogeneic BALB/cJ chimerism was greater than 95% when assessed in PBMC (Fig. 2D) and the

ECI (Fig. 2Ea) and not different between C57BL/6J WT and C57BL/6J GLP-2R KO vehicle or teduglutide-treated mice. Within the ECI, the percentage of allogeneic BALB/cJ CD3+CD8a+ T cells was equivalent in C57BL/6J WT and C57BL/6J GLP-2R KO mice regardless of treatment (70-75% of the CD45+ events) (Fig. 2Eb). Approximately half of those allogeneic T cells were CD69+ and a small fraction were CD69+CD103+ (Fig. 2Ec and 2Ed), contrasting with the >75% double positive CD69+CD103+ tissue retention phenotype [61] characteristic of the residual intraepithelial T cells (~5%) from the C57BL/6J WT and C57BL/6J GLP-2R KO hosts (Fig. 2F).

Intestinal crypt epithelial injury is a hallmark of GvHD in transplant recipients. The crypts house intestinal stem cells (ISCs) and progenitors of the intestinal epithelium and in mice with GvHD, both ISCs and Paneth cells are depleted as they undergo apoptosis driven by pathogenic donor T cell-derived IFNγ[42]. To assess crypt damage, we quantified Paneth cells (identified by their eosinophilic granules) and apoptotic bodies/crypt in H&E-stained ileum sections, alongside measuring *Lyz1* mRNA expression, a Paneth cell marker.

As shown in Fig. 3A and illustrated by representative images in Fig. 3B, mucosal damage in the ileum was similarly severe in both allogeneic C57BL/6J WT and C57BL/6J GLP-2R KO mice and was significantly greater than in syngeneic controls. This was evidenced by reduced Paneth cell counts and *Lyz1* mRNA expression, coupled with a concurrent increase of apoptotic bodies/crypt, consistent with crypt epithelial cell loss. However, no differences were observed in either genotype with teduglutide treatment. Consistent with its intestinotrophic effects, teduglutide treatment significantly increased small intestine weight-to-length ratio and villus height in allogeneic C57BL/6J WT mice, whereas no such changes were observed in allogeneic C57BL/6J GLP-2R KO mice (Fig. 3C). Notably, crypt depth remained unchanged across allogeneic groups (Fig. 3C). We also examined the expression of several IE mRNA transcripts after a single injection of vehicle or teduglutide to allogeneic mice 1 hour before sacrifice. As shown in Fig. 3D, mRNA transcripts for *Egr1*, *Phlda1*, *Areg* and *Ereg* were significantly upregulated in the jejunum of teduglutide-treated C57BL/6J WT mice, but not in their C57BL/6J GLP-2R KO

counterparts. The histomorphometry and gene expression data (Fig. 3C and D) confirm that teduglutide retains its biological activity in the setting of aGvHD.

As shown in Fig. 3E, qPCR analysis confirmed the presence of *Glp2r* exons 7-8 in RNA extracted from the ileum of C57BL/6J WT mice, while no signal was detected in ileum RNA from C57BL/6J GLP-2R KO mice. *Glp2r* mRNA levels were not different between syngeneic and allogeneic C57BL/6J WT mice. Expression levels of mRNA biomarkers for the ISC compartment (*Lgr5*) and epithelial secretory lineages (*Tff3* and *Gcg*) were similar across syngeneic and allogeneic groups, with no differences observed between vehicle- and teduglutide-treated mice (Fig. 3F). In contrast, expression of *Reg3g*, a biomarker of aGvHD severity and gut injury, produced by multiple epithelial lineages[62], was consistently reduced in both C57BL/6J WT and C57BL/6J GLP-2R KO allogeneic mice compared to syngeneic controls (Fig. 3F).

Although ISCs are known to be depleted in mice with GvHD[42], the expression of *Lgr5*, considered a specific ISC mRNA biomarker [63], trended lower in allogeneic mice but the difference was not significant relative to the syngeneic group (Fig. 3F). This unexpected discrepancy may be due to the contribution of villus tip telocytes, which also express *Lgr5* mRNA in whole tissue ileum samples [64]. To unequivocally assess the occurrence of Lgr5+ ISCs in aGvHD, we used reporter B6.129P2-*Lgr5*$^{tm1(cre/ERT2)Cle}$/J (Lgr5-EGFP^{+}) mice[63] to visualize crypt-resident Lgr5-EGFP^{+} ISCs via green fluorescent protein (GFP) immunohistochemistry (IHC) on intestinal tissue sections.

As outlined in the experimental plan (Fig. 4A), Lgr5-EGFP^{+} mice were treated with vehicle or teduglutide for 4 days before receiving a fully mismatched HCT from BALB/cJ donors, with treatment continuing until sacrifice. Syngeneic controls received HCT from C57BL/6J WT donors. During the six-day period following HCT, both syngeneic and allogeneic Lgr5-EGFP^{+} mice, regardless of treatment, exhibited similar body weight BW loss, although divergence between groups began to emerge by day 6 (Fig. 4B). Mucosal damage in the ileum (assessed by Paneth cell counts, *Lyz1* and *Reg3g* mRNA expression, and crypt apoptotic body incidence) was

comparable between vehicle- and teduglutide-treated allogeneic mice, but significantly greater than in syngeneic controls (Fig. 4C). After 12 days of teduglutide treatment, allogeneic Lgr5-EGFP$^+$ mice showed significant increases in small intestine weight-to-length ratio, villus height, and crypt depth (Fig. 4D). Additionally, acute teduglutide challenge strongly induced IE gene expression in the jejunum of these mice (Fig. 4E), further confirming the biological activity of teduglutide during aGvHD.

A comparable level of *Glp2r* mRNA transcripts was detected in the jejunum of both syngeneic and allogeneic Lgr5-EGFP$^+$ mice, irrespective of teduglutide treatment (Fig. 4F). In contrast, relative to syngeneic Lgr5-EGFP$^+$ mice, *eGFP* reporter mRNA expression in the jejunum was significantly reduced in allogeneic mice, regardless of treatment (Fig. 4G left panel). We also used anti-GFP IHC to quantify the number of Lgr5-EGFP$^+$ crypts per circumference and Lgr5-EGFP$^+$ cells per crypt in jejunal tissue sections (Fig. 4G middle and right panels and representative images in 4H). Both syngeneic and allogeneic mice exhibited fewer Lgr5-EGFP$^+$ events per circumference and per crypt compared to non-irradiated controls, with further reductions observed in the allogeneic group, independent of teduglutide treatment. These observations indicate that chronic teduglutide does not prevent the depletion of crypt compartment Lgr5+ ISCs caused by the combined effect of irradiation and allogeneic T cell-mediated damage in aGvHD.

As illustrated in Figs. 2 and 3, the experimental paradigm studied here closely recapitulates the key pathological features of aGvHD, evident in our BALB/cJ-into-C57BL/6J allogeneic murine model. These include progressive weight loss, elevated circulating cytokines, recruitment of allogeneic T cells into the intestinal crypts, mucosal injury and suppression of the ileal antimicrobial aGvHD biomarker *Reg3g*. Although teduglutide retains its biological activity in the context of aGvHD, chronic activation of the GLP-2R via teduglutide administration, failed to ameliorate the clinical course of disease. Notably, it did not prevent the characteristic crypt epithelial injury associated with aGvHD, as evidenced by the loss of Paneth cells (Fig. 3A and Fig. 4C) and ISCs (Fig. 4G). Concurrent genetic ablation studies of the *Glp2r* (Figs. 2 and 3) further demonstrated that loss of GLP-2R signaling did not impact multiple features of disease severity.

Contrary to expectations, our results diverge from those reported by Norona et al.[27] who observed Paneth cell and ISC protection and a reduction in aGvHD mortality following prophylactic teduglutide treatment in a similar murine aGvHD model. To investigate this potential survival benefit, we performed a BALB/cJ-into-C57BL/6J WT or C57BL/6J GLP-2R KO allogeneic HCT using the same teduglutide treatment schedule described by Norona et al. [27] (Fig. 5A) and monitored BW loss and survival throughout aGvHD progression.

Murine models of GvHD typically exhibit two distinct phases of BW loss: an initial, non-lethal phase occurring 5-10 days post-HCT, followed by a recovery period and a second phase that progresses until death[65]. These phases correspond to two waves of donor CD8+ T cell expansion in allogeneic recipients[66]. Both C57BL/6J WT and C57BL/6J GLP-2R KO allogeneic mice showed similar BW loss profiles up to day 27 (Fig. 5B). Beyond this point the small number of surviving mice, particularly in the C57BL/6J GLP-2R KO group, precluded accurate BW loss curve representation. Importantly, no differences in BW loss were observed between vehicle- and teduglutide-treated C57BL/6J WT or C57BL/6J GLP-2R KO mice. Kaplan-Meier survival analysis (Fig. 5C) revealed no significant differences between vehicle- and teduglutide-treated allogeneic C57BL/6J WT mice. Similarly, survival curves for C57BL/6J GLP-2R KO mice were unaffected by teduglutide treatment. Notably, median survival was significantly shorter in C57BL/6J GLP-2R KO mice compared to their C57BL/6J WT counterparts.

Sustained intestinal barrier loss is a critical driver of both the initiation and propagation of GvHD [67], with the extent of intestinal barrier loss correlating with disease severity in patients and mice with GvHD[68-71]. Interestingly, *Glp2r*$^{-/-}$ mice exhibit significantly increased morbidity and mortality and heightened bacterial translocation in preclinical models of gut injury[72]. Moreover, they have elevated small bowel bacterial load, reduced expression of Paneth cell antimicrobial genes and impaired mucosal bactericidal activity [30].

To investigate whether enhanced bacterial infection contributes to the increased mortality observed in C57BL/6J GLP-2R KO mice during aGvHD, we performed a BALB/cJ-into-C57BL/6J WT or C57BL/6J GLP-2R KO allogeneic HCT using the prophylactic teduglutide treatment

regimen described by Norona et al. [24]. Syngeneic transplants with C57BL/6J WT or C57BL/6J GLP-2R KO donors served as aGvHD-negative control mice (Fig. 5D).

During the shorter five-day period following HCT all groups of mice (syngeneic and allogeneic, C57BL/6J WT and C57BL/6J GLP-2R KO, vehicle- and teduglutide-treated) exhibited similar BW loss (Fig. 5E). As expected, syngeneic mice began to recover BW thereafter, while BW continued to decline in the allogeneic groups (grey shaded areas in Fig. 5E). Importantly, BW loss was comparable between C57BL/6J WT and C57BL/6J GLP-2R KO allogeneic mice, regardless of treatment (Fig. 5E, middle and right panels).

To assess the prevalence of bacterial septicemia, blood samples were collected from the tail vein nine days post-HCT, coinciding with the nadir of the first BW loss phase, and plated on tryptic soy agar (TSA). As shown in Fig. 5F, whereas the incidence of positive bacterial cultures in blood was negligible in syngeneic mice, the number of allogeneic C57BL/6J GLP-2R KO mice exhibiting positive bacterial cultures trended significantly higher ($p \leq 0.05$, Chi-square test for trend) relative to levels in their allogeneic C57BL/6J WT counterparts, and this difference was unaffected by teduglutide treatment. The combined studies presented in Fig. 5 indicate that although genetic disruption of the GLP-2R is dispensable for the immunopathogenesis of murine aGvHD modeled herein, loss of endogenous GLP-2R signalling increases susceptibility to the lethal phase of the disease. This heightened vulnerability may be attributed to impaired gut barrier integrity and increased microbial septicemia, characteristic of the GLP-2R KO phenotype [45].

Given the importance of gut microbiota for the pathophysiology of intestinal GvHD[73], we next performed 16S rRNA sequencing to assess how aGvHD and GLP-2R signaling shape gut bacterial communities. Neither aGvHD, nor genotypes, nor teduglutide significantly altered alpha diversity (observed richness, Chao1, Shannon, Simpson) or beta diversity by principal coordinate analysis (PCoA) (Fig. 6A and B). Differential abundance testing with DESeq2 revealed condition-specific compositional shifts. Compared to syngeneic C57BL/6J WT mice, six genera were relatively less abundant (*Enterococcus*, Alistipes, UCG-005, *Rikenellaceae RC9* gut group,

Bacteroides, *Prevotellaceae* UCG-001) and two were more abundant ([*Eubacterium*] *siraeum* group, *Butyribacter*) in syngeneic C57BL/6J GLP-2R KO mice (Fig. 6C). Induction of aGvHD decreased seven genera (*Clostridium, Dubosiella, Thomasclavelia, Anaerotignum*, *Turicimonas,* GCA-900066575, *Helicobacter*) and increased five (*Roseburia*, *Prevotellaceae* UCG-001, *Acutalibacter,* [*Eubacterium*] *siraeum* group, *Candidatus Arthromitus*) in C57BL/6J WT mice. The increase in the segmented filamentous bacterium *Candidatus Arthromitus* was also identified by LEfSe analysis. In contrast, aGvHD induction only decreased *Anaerotignum* and increased four genera (*Rikenellaceae RC9* gut group, *Prevotellaceae* UCG-001, UCG-005, *Candidatus Arthromitus*) significantly in C57BL/6J GLP-2R KO mice. In C57BL/6J WT mice, teduglutide reversed the aGvHD-associated decrease in *Clostridium* and reduced aGvHD-associated *Acutalibacter*, while also increasing *Butyribacter*. These effects were all lost in C57BL/6J GLP-2R KO mice treated with teduglutide. PICRUSt2 detected no significant functional enrichment in microbial metabolic pathways across conditions.

In the Lgr5-EGFP$^+$ mouse study, non-irradiated Lgr5-EGFP$^+$ mice showed higher alpha (observed richness, Chao1) diversity and a shift in beta diversity than allogeneic Lgr5-EGFP$^+$ mice (Fig. 6D and E), suggesting irradiation-HCT exerts major influence on microbial diversity. Irradiation-HCT reduced *Roseburia* and increased eleven genera; aGVHD induction or teduglutide did alter additional microbial abundance (Fig. 6F). LEfSe analysis did not identify significant biomarkers across these conditions. Notably, allogeneic Lgr5-EGFP$^+$ mice receiving teduglutide displayed widespread reductions in predicted functional annotations related to metabolic pathways (Fig. 6G), an effect not observed in allogeneic C57BL/6J WT mice receiving teduglutide.

4.0 Discussion

Considerable evidence from both preclinical studies [27; 40] and clinical case series[28; 29] supports a therapeutic role for GLP-2R agonism in attenuating the severity of intestinal injury in GvHD. Here we set out to explore the mechanisms of teduglutide action in mice with aGvHD. Surprisingly, we were unable to replicate the therapeutic activity of teduglutide in mice following allogeneic HCT despite using very similar treatment protocols described previously to study the acute phase of aGvHD in mice [27]. However, we identified a heretofore unknown role for basal GLP-2R signaling in aGvHD outcomes using *Glp2r*$^{-/-}$ mice, which exhibited increased mortality and bacteremia following allogeneic transplantation.

Mechanistically, although GLP-1R expression is readily detectable on subsets of T cells [11; 15; 74], including T cells proximate to the site of mucosal injury in aGvHD[34], a functional GLP-2R has not been identified on T cells[75]. Rather, GLP-2 appears to modulate gut immune responses indirectly via induction of thymic stromal lymphopoietin (TSLP) in subepithelial fibroblasts and TSLP in turn upregulates type 2 cytokine production via ILC2 cells [76]. GLP-2 may also control inflammation indirectly by regulating gut barrier function, thereby influencing the extent of bacteremia and endotoxemia following experimental intestinal injury [77; 78]. Our previous studies demonstrated that GLP-2R agonism using teduglutide reduced gut injury and the extent of bacteremia in mice with chemotherapy-induced enteritis [22]. Conversely, *Glp2r*$^{-/-}$ mice exhibited enhanced intestinal injury and increased bacterial translocation after induction of enteritis with indomethacin, findings attributed to defective Paneth cell function[30].

We performed 16S rRNA-seq to examine fecal microbial composition, using the same pipeline that we previously applied to test whether gain or loss of GLP-1R function influences aGvHD disease activity[34]. Although fecal communities have been repeatedly linked to aGVHD risk, barrier injury, and disease outcomes[79; 80], changes in fecal microbial composition may not be directly linked to small-intestinal inflammation in aGVHD models because of anatomical differences and region-specific differences in gut-immune networks. Future analysis of the small-intestinal or cecal microbiome using metagenomic and metatranscriptomic approaches

will more comprehensively characterize region-specific microbial composition and function in this context.

Few studies have examined the impact of GLP-2R signaling on gut microbial profiles. Lethal irradiation drives more pronounced changes in microbial profiles than the induction of aGVHD. *Alistipes* is highly sensitive to global GLP-2R loss and is not rescued by teduglutide. In genera altered by aGvHD induction, teduglutide increases *Clostridium*, consistent with prior findings[81] and decreases *Acutalibacter,* with the effects lost in C57BL/6J GLP-2R KO mice. The dampening effects of teduglutide on multiple microbial metabolic pathways in allogeneic Lgr5-EGFP^{+} mice are notable, given that this effect was absent in allogeneic C57BL/6J mice; this discrepancy could reflect the shorter experimental duration in the Lgr5 reporter study or genetic differences between Lgr5-EGFP^{+} and C57BL/6J backgrounds. Nevertheless, neither gain nor loss of GLP-2R function overtly alters gut microbial communities in the setting of aGvHD, consistent with the absence of anti-inflammatory benefit against intestinal aGvHD.

Our observations of increased mortality and bacteremia in *Glp2r*$^{-/-}$ mice with aGvHD add to the body of experimental evidence highlighting the importance of basal GLP-2R signaling for maintenance of the gut barrier[77], notably in the context of gut injury. Consistent with this notion, *Glp2r*$^{-/-}$ mice display increased mortality and bacteremia following induction of sepsis with cecal puncture[82].

The gastrointestinal actions of GLP-2 and teduglutide to enhance nutrient absorption, promote expansion of the mucosal epithelium, and attenuate gallbladder emptying have been widely replicated in mice, rats and humans[1; 20; 72; 83], supporting the successful development of teduglutide for the treatment of intestinal failure in adults and children with short bowel syndrome[83]. Based in part on more limited preclinical and clinical data linking GLP-2 action to intestinal cytoprotection in aGvHD, a clinical trial was initiated to examine the therapeutic potential of apraglutide, a long-acting GLP-2 analogue, in patients with steroid refractory aGvHD (NCT05415410). However, it appears that the trial was terminated prematurely by the sponsor.

Our inability to replicate the striking therapeutic benefits of GLP-2R agonism in experimental aGvHD[27], suggests that the therapeutic potential and reproducibility of GLP-2R agonists in this translational setting remains uncertain and merits more detailed independent evaluation.

Limitations of these studies

Our protocol sought to replicate previous studies using teduglutide in aGvHD, and it is possible that more chronic studies, using longer-acting and more potent GLP-2 medicines, might have provided more positive results on a wider range of endpoints. Our studies of bacteremia may have underestimate the magnitude of the effect size, due to sampling and culture of tail vein, rather than portal vein blood. It is not clear whether one or more actions of teduglutide required to reduce gut injury are subject to desensitization using the protocol studied here in the murein aGvHD model. Finally, teduglutide is a relatively short-acting GLP-2R agonist, and it remains possible that newer agents with optimized pharmacokinetics profiles administered for more extended time periods might exhibit greater therapeutic efficacy in preclinical and clinical studies of aGvHD.

Acknowledgments

DJD is supported by a Banting and Best Diabetes Centre Novo Nordisk Chair in Incretin Biology, a Sinai Health-Novo Nordisk Foundation Chair in Regulatory Peptides, CIHR grants 154321 and 192044 and Diabetes Canada-Canadian Cancer Society Grant OG-3- 24-5819-DD.

Figure Legends

Fig 1. Bone marrow-derived cells do not mediate teduglutide-dependent effects in the gut after HCT. (A) Schematic of the experimental design. Bone marrow chimeras were created using congenic Pep Boy mice as donors and C57BL/6J WT (C57 WT) (n=14) or C57BL/6J GLP-2R KO (C57 KO) (n=14) mice as recipients. After confirming the extent of chimerism by flow cytometry on PBMC 1-month post-transplantation **(B)**, the recipient mice were treated for 9 days with vehicle (Veh) (n=7 C57BL/6J WT and C57BL/6J GLP-2R KO) or teduglutide (Tedu) (n=7 C57BL/6J WT and C57BL/6J GLP-2R KO). **(C)** Small intestinal weight to length ratio and jejunal villus height and crypt depth. **(D** and **E)** mRNA expression of the indicated transcripts measured by qPCR in jejunum from mice treated with teduglutide 200 µg/kg 1 hour before sacrifice. ND, not detectable. PBMC=Peripheral Blood Mononuclear Cell. Data are mean ± SD pooled from 2 independent experiments from the same cohort of mice. $^{**}p \leq 0.01$, $^{***}p \leq 0.001$ and $^{****}p \leq 0.0001$ by 2-way ANOVA followed by Tukey's multiple comparisons tests.

Fig 2. Chronic teduglutide treatment or genetic disruption of the GLP-2R does not affect body weight loss, systemic cytokine storm, or recruitment of allogeneic T cells to the gut during aGvHD. (A) Schematic of the experimental design. C57BL/6J WT (C57 WT) and C57BL/6J GLP-2R KO (C57 KO) mice were treated with vehicle (Veh) or teduglutide (Tedu) for 4 days before undergoing HCT from syngeneic (Syn) donors (C57BL/6J WT n=5 and C57BL/6J GLP-2R KO n=3) or allogeneic (Allo) BALB/cJ donors (C57BL/6J WT n=6 Veh and 4 Tedu and C57BL/6J GLP-2R KO n=7 Veh and 7 Tedu) and treatment continued until sacrifice. **(B)** Sequence of body weight loss during the experiment. The grey shaded areas are a visual reference to compare the body weight decline in allogeneic mice relative to the syngeneic group indicative of the aGvHD progress. **(C)** Plasma cytokine levels. (**D** and **E**) Chimerism assessed at the time of sacrifice by flow cytometry on **(D)** PBMC and on **(E** and **F)** small intestine epithelial compartment-associated immune cells (ECI) isolated from allogeneic recipient mice (C57BL/6J WT n=4 Veh and 3 Tedu, C57BL/6J GLP-2R KO n=4 Veh and 5 Tedu). WT=wildtype, KO=knockout. Data are mean ± SD pooled from 2 independent experiments from the same cohort of mice. $^{*}p \leq 0.05$, $^{**}p \leq 0.01$ and $^{****}p \leq 0.0001$ by 2-way ANOVA followed by Tukey's multiple comparisons tests.

Fig 3. Chronic teduglutide treatment or genetic disruption of the GLP-2R does not modify the characteristic intestinal tissue damage associated with aGvHD development. Panels **A** to **F** are a continuation of subsequent analyses linked to the experiment described in **Fig 2A**. **(A)** Number of Paneth cells/crypt, *lysozyme 1* mRNA expression measured by qPCR, and number of apoptotic bodies/crypt in ileum. **(B)** Representative crypt images from ileum sections stained with H&E. Arrowheads indicate crypt epithelium apoptotic cells. **(C)** Small intestinal weight to length ratio and jejunal villus height and crypt depth. **(D)** Expression of the indicated mRNA transcripts measured by qPCR in jejunum following an acute 200 µg/kg teduglutide (Tedu) challenge 1 hour before sacrifice. **(E)** mRNA expression of *Glp2r* and **(F)** select epithelial cell lineages measured by qPCR in ileum. ND, not detectable. Data are mean ± SD pooled from 2 independent experiments from the same cohort of mice. **p* ≤0.05, ***p* ≤0.01, ****p* ≤0.001 and *****p* ≤0.0001 by 2-way ANOVA followed by Tukey's multiple comparisons tests.

Fig 4. Chronic teduglutide treatment does not prevent the loss of Lgr5-EGFP$^+$ intestinal stem cells during aGvHD. (A) Schematic of the experimental design. Lgr5-EGFP$^+$ mice were treated with vehicle (Veh) or teduglutide (Tedu) for 4 days before undergoing HCT from syngeneic (Syn) C57BL/6J WT donors (Lgr5-EGFP$^+$ n=7) or allogeneic (Allo) BALB/cJ donors (n=8 Lgr5-EGFP$^+$ Veh and 8 Tedu) and treatment continued until sacrifice. Vehicle treated non-irradiated (NI) Lgr5-EGFP$^+$ mice (n=6) cohoused with syngeneic and allogeneic mice were used in middle and right panels **G** and in panel **H** for both baseline gene expression comparisons and as positive control for scoring GFP+ crypts. **(B)** Serial body weight loss during the experiment. The grey shaded areas are a visual reference to compare body weight in allogeneic mice relative to the syngeneic group. **(C)** Number of Paneth cells/crypt, *lysozyme 1* and *Reg3g* mRNA expression measured by qPCR and number of apoptotic bodies/crypt in ileum. **(D)** Small intestinal weight to length ratio and jejunal villus height and crypt depth. **(E)** Expression of the indicated mRNA transcripts measured by qPCR in jejunum following an acute 200 µg/kg teduglutide challenge 1 hour before sacrifice. **(F)** mRNA expression of *Glp2r* measured by qPCR in jejunum. **(G)** mRNA expression of *eGFP* measured by qPCR (left panel) and number of GFP+ crypts/cross sectional circumference and GFP+ cells/crypt (middle and right panels) in jejunum. **(H)** Representative crypt images from

jejunum sections stained with an anti-GFP antibody. Data are mean ± SD pooled from 2 independent experiments from 2 independent cohorts of mice. *$p \leq 0.05$, **$p \leq 0.01$, ***$p \leq 0.001$ and ****$p \leq 0.0001$ by Student's t tests (only panels **D** and **E**) and by 2-way ANOVA followed by Tukey's multiple comparisons tests.

Fig 5. Prophylactic teduglutide treatment does not improve survival in mice undergoing aGvHD whereas loss-of-function of the GLP-2R significantly shortens median survival. (A) Schematic of the experimental design. C57BL/6J WT (C57 WT) and C57BL/6J GLP-2R KO (C57 KO) mice were treated with vehicle (Veh) or teduglutide (Tedu) 3 days before and 3 days after HCT from allogeneic (Allo) BALB/cJ donors (C57BL/6J WT n=13 Veh and 15 Tedu and C57BL/6J GLP-2R KO n=20 Veh and 8 Tedu). **(B)** Sequence of body weight loss during the experiment. The grey checkered areas are a visual reference to compare body weight decline in allogeneic mice during the lethal phase of aGvHD. Data are mean ± SD **(C)** Kaplan-Meier survival proportion plots of C57BL/6J WT and C57BL/6J GLP-2R KO allogeneic mice. The Log-rank (Mantel-Cox) test indicated a significant difference (****$p \leq 0.0001$) in the survival curves between C57BL/6J WT and C57BL/6J GLP-2R KO mice. Data are combined from 4 independent experiments from 2 independent cohorts of mice. **(D)** Schematic of the experimental design. C57BL/6J WT (C57 WT) and C57BL/6J GLP-2R KO (C57 KO) mice were treated with vehicle (Veh) or teduglutide (Tedu) 3 days before and 3 days after HCT from syngeneic (Syn) donors (C57BL/6J WT n=5 and C57BL/6J GLP-2R KO n=5) or allogeneic (Allo) BALB/cJ donors (C57BL/6J WT n=9 Veh and 9 Tedu and C57BL/6J GLP-2R KO n=9 Veh and 9 Tedu). **(E)** Sequence of body weight loss during the experiment (mean ± SD). The grey shaded areas are a visual reference to compare the body weight decline in allogeneic mice relative to the syngeneic group indicative of aGvHD progress. **(F)** Tail blood bacteremia. *$p \leq 0.05$ by Chi-square test for trend. Data are pooled from 2 independent experiments from the same cohort of mice.

Figure 6. GLP-2R signaling modulates specific gut microbiota taxa during aGvHD. (A) Alpha diversity (Observed, Chao, Shannon and Simpson) of gut microbiota in C57BL/6J WT or C57BL/6J GLP2R KO mice receiving HCT from syngeneic donors (Syn) or from allogeneic BALB/cJ donors (Allo) and treated with vehicle (Veh) or teduglutide (Tedu) from 4 days before HCT until sacrifice.

(B) Principal Coordinates Analysis (PCoA) of Bray-Curtis dissimilarity for microbiota profiles from the mice in **(A)**. **(C)** Heatmap showing relative abundance of genera significantly altered across aGvHD induction, genotypes, and teduglutide treatment. **(D)** Alpha diversity (Observed, Chao, Shannon and Simpson) of gut microbiota in non-irradiated Lgr5-EGFP^{+} mice (Lgr5 NI), syngeneic Lgr5-EGFP^{+} mice (Lgr5 Syn), and allogeneic Lgr5-EGFP^{+} mice treated with vehicle (Lgr5 Allo + Vehicle) or teduglutide (Lgr5 Allo + Tedu) from 4 days before HCT until sacrifice. **(E)** PCoA of Bray-Curtis dissimilarity of microbiota profiles from the mice in **(D)**. **(F)** Heatmap showing relative abundance of genera significantly altered between Lgr5 NI mice and groups receiving HCT. The dashed line indicates genera with higher vs. lower abundance in Lgr5 NI relative to Lgr5 Syn. **(G)** Heatmap showing predicted metabolic pathways with differential functional abundance between Lgr5 Allo + Vehicle and Lgr5 Allo + Tedu groups. Statistical significance was determined by Kruskal-Wallis test with false discovery rate correction in **H**, and by DESeq2 with multiple testing correction in **D**.

[1] Brubaker, P.L., 2022. The Molecular Determinants of Glucagon-like Peptide Secretion by the Intestinal L cell. Endocrinology 163(11).
[2] Drucker, D.J., Habener, J.F., Holst, J.J., 2017. Discovery, characterization, and clinical development of the glucagon-like peptides. J Clin Invest 127(12):4217-4227.
[3] Drucker, D.J., Holst, J.J., 2023. The expanding incretin universe: from basic biology to clinical translation. Diabetologia 66(10):1765-1779.
[4] Campbell, J.E., Muller, T.D., Finan, B., DiMarchi, R.D., Tschop, M.H., D'Alessio, D.A., 2023. GIPR/GLP-1R dual agonist therapies for diabetes and weight loss-chemistry, physiology, and clinical applications. Cell Metab 35(9):1519-1529.
[5] Muller, T.D., Finan, B., Bloom, S.R., D'Alessio, D., Drucker, D.J., Flatt, P.R., et al., 2019. Glucagon-like peptide 1 (GLP-1). Mol Metab 30:72-130.
[6] Drucker, D.J., Yusta, B., 2014. Physiology and pharmacology of the enteroendocrine hormone glucagon-like peptide-2. Annu Rev Physiol 76:561-583.
[7] Funayama, T., Nozu, T., Ishioh, M., Igarashi, S., Tanaka, H., Sumi, C., et al., 2025. Splenectomy prevents brain orexin, ghrelin, or oxytocin but not GLP-1-induced improvement of intestinal barrier function in rats. Neurogastroenterol Motil 37(2):e14949.
[8] Voetmann, L.M., Underwood, C.R., Rolin, B., Hansen, A.K., Kirk, R.K., Pyke, C., et al., 2022. In vitro cell cultures of Brunner's glands from male mouse to study GLP-1 receptor function. Am J Physiol Cell Physiol 322(6):C1260-C1269.
[9] Bang-Berthelsen, C.H., Holm, T.L., Pyke, C., Simonsen, L., Sokilde, R., Pociot, F., et al., 2016. GLP-1 Induces Barrier Protective Expression in Brunner's Glands and Regulates Colonic Inflammation. Inflamm Bowel Dis 22(9):2078-2097.
[10] Lebrun, L.J., Lenaerts, K., Kiers, D., Pais de Barros, J.P., Le Guern, N., Plesnik, J., et al., 2017. Enteroendocrine L Cells Sense LPS after Gut Barrier Injury to Enhance GLP-1 Secretion. Cell Rep 21(5):1160-1168.
[11] Wong, C.K., Yusta, B., Koehler, J.A., Baggio, L.L., McLean, B.A., Matthews, D., et al., 2022. Divergent roles for the gut intraepithelial lymphocyte GLP-1R in control of metabolism, microbiota, and T cell-induced inflammation. Cell Metab 34(10):1514-1531 e1517.
[12] Su, Y., Liu, N., Zhang, Z., Li, H., Ma, J., Yuan, Y., et al., 2022. Cholecystokinin and glucagon-like peptide-1 analogues regulate intestinal tight junction, inflammation, dopaminergic neurons and alpha-synuclein accumulation in the colon of two Parkinson's disease mouse models. Eur J Pharmacol 926:175029.
[13] Wang, W., Zhang, C., Zhang, H., Li, L., Fan, T., Jin, Z., 2023. The alleviating effect and mechanism of GLP-1 on ulcerative colitis. Aging (Albany NY) 15(16):8044-8060.
[14] Sun, H., Shu, J., Tang, J., Li, Y., Qiu, J., Ding, Z., et al., 2024. GLP-1 receptor agonists alleviate colonic inflammation by modulating intestinal microbiota and the function of group 3 innate lymphoid cells. Immunology 172(3):451-468.
[15] Yusta, B., Baggio, L.L., Koehler, J., Holland, D., Cao, X., Pinnell, L.J., et al., 2015. GLP-1 receptor (GLP-1R) agonists modulate enteric immune responses through the intestinal intraepithelial lymphocyte (IEL) GLP-1R. Diabetes 64(7):2537-2549.
[16] Sorum, M.E., Gang, A.O., Tholstrup, D.M., Gudbrandsdottir, S., Kissow, H., Kornblit, B., et al., 2024. Semaglutide treatment for PRevention Of Toxicity in high-dosE Chemotherapy with autologous haematopoietic stem-cell Transplantation (PROTECT): study protocol for a randomised, double-blind, placebo-controlled, investigator-initiated study. BMJ Open 14(10):e089862.
[17] Benjamin, M.A., McKay, D.M., Yang, P.C., Cameron, H., Perdue, M.H., 2000. Glucagon-like peptide-2 enhances intestinal epithelial barrier function of both transcellular and paracellular pathways in the mouse. Gut 47(1):112-119.

[18] Cameron, H.L., Yang, P.C., Perdue, M.H., 2003. Glucagon-like peptide-2-enhanced barrier function reduces pathophysiology in a model of food allergy. Am J Physiol Gastrointest Liver Physiol 284(6):G905-G912.
[19] Maruta, K., Takajo, T., Akiba, Y., Said, H., Irie, E., Kato, I., et al., 2020. GLP-2 Acutely Prevents Endotoxin-Related Increased Intestinal Paracellular Permeability in Rats. Dig Dis Sci 65(9):2605-2618.
[20] Drucker, D.J., Erlich, P., Asa, S.L., Brubaker, P.L., 1996. Induction of intestinal epithelial proliferation by glucagon-like peptide 2. Proc Natl Acad Sci U S A 93(15):7911-7916.
[21] Boushey, R.P., Yusta, B., Drucker, D.J., 1999. Glucagon-like peptide 2 decreases mortality and reduces the severity of indomethacin-induced murine enteritis. Am J Physiol 277:E937-E947.
[22] Boushey, R.P., Yusta, B., Drucker, D.J., 2001. Glucagon-like peptide (GLP)-2 reduces chemotherapy-associated mortality and enhances cell survival in cells expressing a transfected GLP-2 receptor. Cancer Res 61(2):687-693.
[23] Drucker, D.J., Yusta, B., Boushey, R.P., DeForest, L., Brubaker, P.L., 1999. Human [Gly2]GLP-2 reduces the severity of colonic injury in a murine model of experimental colitis. Am J Physiol 276(1):G79-91.
[24] Li, D., Gao, Y., Cui, L., Li, Y., Ling, H., Tan, X., et al., 2023. Integrative analysis revealed the role of glucagon-like peptide-2 in improving experimental colitis in mice by inhibiting inflammatory pathways, regulating glucose metabolism, and modulating gut microbiota. Front Microbiol 14:1174308.
[25] Chandwe, K., Bwakura-Dangarembizi, M., Amadi, B., Tawodzera, G., Ngosa, D., Dzikiti, A., et al., 2024. Malnutrition enteropathy in Zambian and Zimbabwean children with severe acute malnutrition: A multi-arm randomized phase II trial. Nat Commun 15(1):2910.
[26] Buchman, A.L., Katz, S., Fang, J.C., Bernstein, C.N., Abou-Assi, S.G., Teduglutide Study, G., 2010. Teduglutide, a novel mucosally active analog of glucagon-like peptide-2 (GLP-2) for the treatment of moderate to severe Crohn's disease. Inflamm Bowel Dis 16(6):962-973.
[27] Norona, J., Apostolova, P., Schmidt, D., Ihlemann, R., Reischmann, N., Taylor, G., et al., 2020. Glucagon-like peptide 2 for intestinal stem cell and Paneth cell repair during graft-versus-host disease in mice and humans. Blood 136(12):1442-1455.
[28] Ramos, K.N., Leino, D., Luebbering, N., Grimley, M.S., Badia, P., Davies, S.M., et al., 2024. Use of Teduglutide in the Management of Gastrointestinal Graft-versus-Host Disease in Children and Young Adults. Transplant Cell Ther 30(4):454 e451-454 e456.
[29] Brehm, N., Biavasco, F., Clausen, J., Jung, J., Maas-Bauer, K., Wasch, R., et al., 2025. Teduglutide for treatment-refractory severe intestinal acute graft-versus-host disease - a multicenter survey. Bone Marrow Transplant 60(6):873-878.
[30] Lee, S.J., Lee, J., Li, K.K., Holland, D., Maughan, H., Guttman, D.S., et al., 2012. Disruption of the murine Glp2r impairs Paneth cell function and increases susceptibility to small bowel enteritis. Endocrinology 153(3):1141-1151.
[31] Han, S., Liang, C.P., DeVries-Seimon, T., Ranalletta, M., Welch, C.L., Collins-Fletcher, K., et al., 2006. Macrophage insulin receptor deficiency increases ER stress-induced apoptosis and necrotic core formation in advanced atherosclerotic lesions. Cell Metab 3(4):257-266.
[32] Pujadas, G., Varin, E.M., Baggio, L.L., Mulvihill, E.E., Bang, K.W.A., Koehler, J.A., et al., 2020. The gut hormone receptor GIPR links energy availability to the control of hematopoiesis. Mol Metab 39:101008.
[33] Hammoud, R., Kaur, K.D., Koehler, J.A., Baggio, L.L., Wong, C.K., Advani, K.E., et al., 2024. Glucose-dependent insulinotropic polypeptide receptor signaling alleviates gut inflammation in mice. JCI Insight 10(3).
[34] Yusta, B., Wong, C.K., Matthews, D., Koehler, J.A., Baggio, L.L., Bang, K.A., et al., 2025. GLP-1R signaling does not modify the severity of experimental graft versus host disease. Mol Metab 100:102235.

[35] Callahan, B.J., McMurdie, P.J., Rosen, M.J., Han, A.W., Johnson, A.J., Holmes, S.P., 2016. DADA2: High-resolution sample inference from Illumina amplicon data. Nat Methods 13(7):581-583.
[36] McMurdie, P.J., Holmes, S., 2013. phyloseq: an R package for reproducible interactive analysis and graphics of microbiome census data. PLoS One 8(4):e61217.
[37] Love, M.I., Huber, W., Anders, S., 2014. Moderated estimation of fold change and dispersion for RNA-seq data with DESeq2. Genome Biol 15(12):550.
[38] Segata, N., Izard, J., Waldron, L., Gevers, D., Miropolsky, L., Garrett, W.S., et al., 2011. Metagenomic biomarker discovery and explanation. Genome Biol 12(6):R60.
[39] Douglas, G.M., Maffei, V.J., Zaneveld, J.R., Yurgel, S.N., Brown, J.R., Taylor, C.M., et al., 2020. PICRUSt2 for prediction of metagenome functions. Nat Biotechnol 38(6):685-688.
[40] Minden, M.D., Audiger, C., Chabot-Roy, G., Lesage, S., Delisle, J.S., Biemans, B., et al., 2024. The Long-Acting Glucagon-Like Peptide-2 Analog Apraglutide Enhances Intestinal Protection and Survival After Chemotherapy and Allogeneic Transplantation in Mice. Ann Transplant 29:e945249.
[41] Fu, Y.Y., Egorova, A., Sobieski, C., Kuttiyara, J., Calafiore, M., Takashima, S., et al., 2019. T Cell Recruitment to the Intestinal Stem Cell Compartment Drives Immune-Mediated Intestinal Damage after Allogeneic Transplantation. Immunity 51(1):90-103 e103.
[42] Takashima, S., Martin, M.L., Jansen, S.A., Fu, Y., Bos, J., Chandra, D., et al., 2019. T cell-derived interferon-gamma programs stem cell death in immune-mediated intestinal damage. Sci Immunol 4(42).
[43] Rodic, N., Rutenberg, M.S., Terada, N., 2004. Cell fusion and reprogramming: resolving our transdifferences. Trends Mol Med 10(3):93-96.
[44] Rizvi, A.Z., Swain, J.R., Davies, P.S., Bailey, A.S., Decker, A.D., Willenbring, H., et al., 2006. Bone marrow-derived cells fuse with normal and transformed intestinal stem cells. Proc Natl Acad Sci U S A 103(16):6321-6325.
[45] Bonde, S., Pedram, M., Stultz, R., Zavazava, N., 2010. Cell fusion of bone marrow cells and somatic cell reprogramming by embryonic stem cells. FASEB J 24(2):364-373.
[46] Pedone, E., Olteanu, V.A., Marucci, L., Munoz-Martin, M.I., Youssef, S.A., de Bruin, A., et al., 2017. Modeling Dynamics and Function of Bone Marrow Cells in Mouse Liver Regeneration. Cell Rep 18(1):107-121.
[47] Johansson, C.B., Youssef, S., Koleckar, K., Holbrook, C., Doyonnas, R., Corbel, S.Y., et al., 2008. Extensive fusion of haematopoietic cells with Purkinje neurons in response to chronic inflammation. Nat Cell Biol 10(5):575-583.
[48] Nygren, J.M., Liuba, K., Breitbach, M., Stott, S., Thoren, L., Roell, W., et al., 2008. Myeloid and lymphoid contribution to non-haematopoietic lineages through irradiation-induced heterotypic cell fusion. Nat Cell Biol 10(5):584-592.
[49] Davies, P.S., Powell, A.E., Swain, J.R., Wong, M.H., 2009. Inflammation and proliferation act together to mediate intestinal cell fusion. PLoS One 4(8):e6530.
[50] Yusta, B., Huang, L., Munroe, D., Wolff, G., Fantaske, R., Sharma, S., et al., 2000. Enteroendocrine localization of GLP-2 receptor expression. Gastroenterology 119(3):744-755.
[51] Guan, X., Karpen, H.E., Stephens, J., Bukowski, J.T., Niu, S., Zhang, G., et al., 2006. GLP-2 receptor localizes to enteric neurons and endocrine cells expressing vasoactive peptides and mediates increased blood flow. Gastroenterology 130(1):150-164.
[52] Orskov, C., Hartmann, B., Poulsen, S.S., Thulesen, J., Hare, K.J., Holst, J.J., 2005. GLP-2 stimulates colonic growth via KGF, released by subepithelial myofibroblasts with GLP-2 receptors. Regul Pept 124(1-3):105-112.
[53] Pedersen, J., Pedersen, N.B., Brix, S.W., Grunddal, K.V., Rosenkilde, M.M., Hartmann, B., et al., 2015. The glucagon-like peptide 2 receptor is expressed in enteric neurons and not in the epithelium of the intestine. Peptides 67:20-28.

[54] Kaestner, K., Zhu, G., Lahori, D., Schug, J., 2024. Villification of the intestinal epithelium is driven by Foxl1. Res Sq.
[55] Drucker, D.J., Shi, Q., Crivici, A., Sumner-Smith, M., Tavares, W., Hill, M., et al., 1997. Regulation of the biological activity of glucagon-like peptide 2 in vivo by dipeptidyl peptidase IV. Nat Biotechnol 15(7):673-677.
[56] Yusta, B., Holland, D., Koehler, J.A., Maziarz, M., Estall, J.L., Higgins, R., et al., 2009. ErbB signaling is required for the proliferative actions of GLP-2 in the murine gut. Gastroenterology 173(3):986-996.
[57] Hill, G.R., Koyama, M., 2020. Cytokines and costimulation in acute graft-versus-host disease. Blood 136(4):418-428.
[58] Fajgenbaum, D.C., June, C.H., 2020. Cytokine Storm. N Engl J Med 383(23):2255-2273.
[59] Deeg, H.J., Storb, R., 1986. Acute and chronic graft-versus-host disease: clinical manifestations, prophylaxis, and treatment. J Natl Cancer Inst 76(6):1325-1328.
[60] Nikolic, B., Lee, S., Bronson, R.T., Grusby, M.J., Sykes, M., 2000. Th1 and Th2 mediate acute graft-versus-host disease, each with distinct end-organ targets. J Clin Invest 105(9):1289-1298.
[61] Kok, L., Masopust, D., Schumacher, T.N., 2022. The precursors of CD8(+) tissue resident memory T cells: from lymphoid organs to infected tissues. Nat Rev Immunol 22(5):283-293.
[62] Zhao, D., Kim, Y.H., Jeong, S., Greenson, J.K., Chaudhry, M.S., Hoepting, M., et al., 2018. Survival signal REG3alpha prevents crypt apoptosis to control acute gastrointestinal graft-versus-host disease. J Clin Invest 128(11):4970-4979.
[63] Barker, N., van Es, J.H., Kuipers, J., Kujala, P., van den Born, M., Cozijnsen, M., et al., 2007. Identification of stem cells in small intestine and colon by marker gene Lgr5. Nature 449(7165):1003-1007.
[64] Bahar Halpern, K., Massalha, H., Zwick, R.K., Moor, A.E., Castillo-Azofeifa, D., Rozenberg, M., et al., 2020. Lgr5+ telocytes are a signaling source at the intestinal villus tip. Nat Commun 11(1):1936.
[65] van Leeuwen, L., Guiffre, A., Atkinson, K., Rainer, S.P., Sewell, W.A., 2002. A two-phase pathogenesis of graft-versus-host disease in mice. Bone Marrow Transplant 29(2):151-158.
[66] Li, X., Deng, R., He, W., Liu, C., Wang, M., Young, J., et al., 2012. Loss of B7-H1 expression by recipient parenchymal cells leads to expansion of infiltrating donor CD8+ T cells and persistence of graft-versus-host disease. J Immunol 188(2):724-734.
[67] Nalle, S.C., Zuo, L., Ong, M., Singh, G., Worthylake, A.M., Choi, W., et al., 2019. Graft-versus-host disease propagation depends on increased intestinal epithelial tight junction permeability. J Clin Invest 129(2):902-914.
[68] Nalle, S.C., Kwak, H.A., Edelblum, K.L., Joseph, N.E., Singh, G., Khramtsova, G.F., et al., 2014. Recipient NK cell inactivation and intestinal barrier loss are required for MHC-matched graft-versus-host disease. Sci Transl Med 6(243):243ra287.
[69] de Mooij, C.E.M., Netea, M.G., van der Velden, W., Blijlevens, N.M.A., 2017. Targeting the interleukin-1 pathway in patients with hematological disorders. Blood 129(24):3155-3164.
[70] Lounder, D.T., Khandelwal, P., Dandoy, C.E., Jodele, S., Grimley, M.S., Wallace, G., et al., 2017. Lower levels of vitamin A are associated with increased gastrointestinal graft-versus-host disease in children. Blood 129(20):2801-2807.
[71] Noth, R., Lange-Grumfeld, J., Stuber, E., Kruse, M.L., Ellrichmann, M., Hasler, R., et al., 2011. Increased intestinal permeability and tight junction disruption by altered expression and localization of occludin in a murine graft versus host disease model. BMC Gastroenterol 11:109.
[72] Drucker, D.J., 2019. The discovery of GLP-2 and development of teduglutide for short bowel syndrome. ACS Pharmacology and Translational Science March DOI: 10.1021/acsptsci.1029b00016.

[73] Fredricks, D.N., 2019. The gut microbiota and graft-versus-host disease. J Clin Invest 129(5):1808-1817.
[74] Wong, C.K., Yusta, B., Tong, J.C.L., Broichhagen, J., Hodson, D.J., Drucker, D.J., 2025. Reassessment of antibody-based detection of the murine T cell GLP-1 receptor. Cell Metab 37(9):1783-1788.
[75] Heng, T.S., Painter, M.W., Immunological Genome Project, C., 2008. The Immunological Genome Project: networks of gene expression in immune cells. Nat Immunol 9(10):1091-1094.
[76] Liao, C., Ji, M., Wang, Z.E., Drucker, D.J., Liang, H.E., Locksley, R.M., 2024. Telocytes link epithelial nutrient sensing with amplification of the ILC2-tuft cell circuit. bioRxiv.
[77] Cani, P.D., Possemiers, S., Van de Wiele, T., Guiot, Y., Everard, A., Rottier, O., et al., 2009. Changes in gut microbiota control inflammation in obese mice through a mechanism involving GLP-2-driven improvement of gut permeability. Gut 58(8):1091-1103.
[78] Kouris, G.J., Liu, Q., Rossi, H., Djuricin, G., Gattuso, P., Nathan, C., et al., 2001. The effect of glucagon-like peptide 2 on intestinal permeability and bacterial translocation in acute necrotizing pancreatitis. Am J Surg 181(6):571-575.
[79] Bowerman, K.L., Varelias, A., Lachner, N., Kuns, R.D., Hill, G.R., Hugenholtz, P., 2020. Continuous pre- and post-transplant exposure to a disease-associated gut microbiome promotes hyper-acute graft-versus-host disease in wild-type mice. Gut Microbes 11(4):754-770.
[80] Koyama, M., Hippe, D.S., Srinivasan, S., Proll, S.C., Miltiadous, O., Li, N., et al., 2023. Intestinal microbiota controls graft-versus-host disease independent of donor-host genetic disparity. Immunity 56(8):1876-1893 e1878.
[81] Hu, X., Cheng, W., Fan, S., Huang, Y., Chen, X., Jiang, Z., et al., 2021. Therapeutic potential of an intestinotrophic hormone, glucagon-like peptide 2, for treatment of type 2 short bowel syndrome rats with intestinal bacterial and fungal dysbiosis. BMC Infect Dis 21(1):583.
[82] Kahles, F., Mertens, R., Diebold, S., Arrivas, M.C., Moellmann, J., Steitz, J., et al., 2022. GLP-2 as an indicator and modulator of acute inflammation improves cardiac function and survival in sepsis. European Heart Journal 43(Supplement_2).
[83] Gasbjerg, L.S., Nielsen, C.K., Suppli, M.P., Grondahl, M.F.G., Holst, J.J., Knop, F.K., et al., 2026. Proglucagon-derived peptides: human physiology and therapeutic potential. Physiol Rev 106(1):529-586.

Upregulation of gene expression and mucosal growth by GLP-2 is preserved in GvHD

Teduglutide does not rescue mortality or reduce inflammation in mice with GvHD

GLP-2R-dependent changes in gut microbial profiles are modest in mice with GvHD

Loss of GLP-2R signaling increases mortality and bacteremia in Glp2r-/- mice with GvHD

Declaration of interests

☐The authors declare that they have no known competing financial interests or personal relationships that could have appeared to influence the work reported in this paper.

☒The authors declare the following financial interests/personal relationships which may be considered as potential competing interests:

Daniel Drucker reports a relationship with D.J.D. has received consulting fees from Amgen, AstraZeneca Inc, Alnylam, Crinetics Eli Lilly Inc, Insulet, Kallyope, Metsara and Pfizer Inc. that includes: consulting or advisory. Daniel Drucker reports a relationship with Amgen, Eli Lilly Inc, Novo Nordisk, and Zealand Pharmaceuticals Inc that includes: funding grants. Daniel Drucker has patent #GLP-2 patent portfolio with royalties paid to Takeda. Member, Editorial Board, Molecular Metabolism If there are other authors, they declare that they have no known competing financial interests or personal relationships that could have appeared to influence the work reported in this paper.

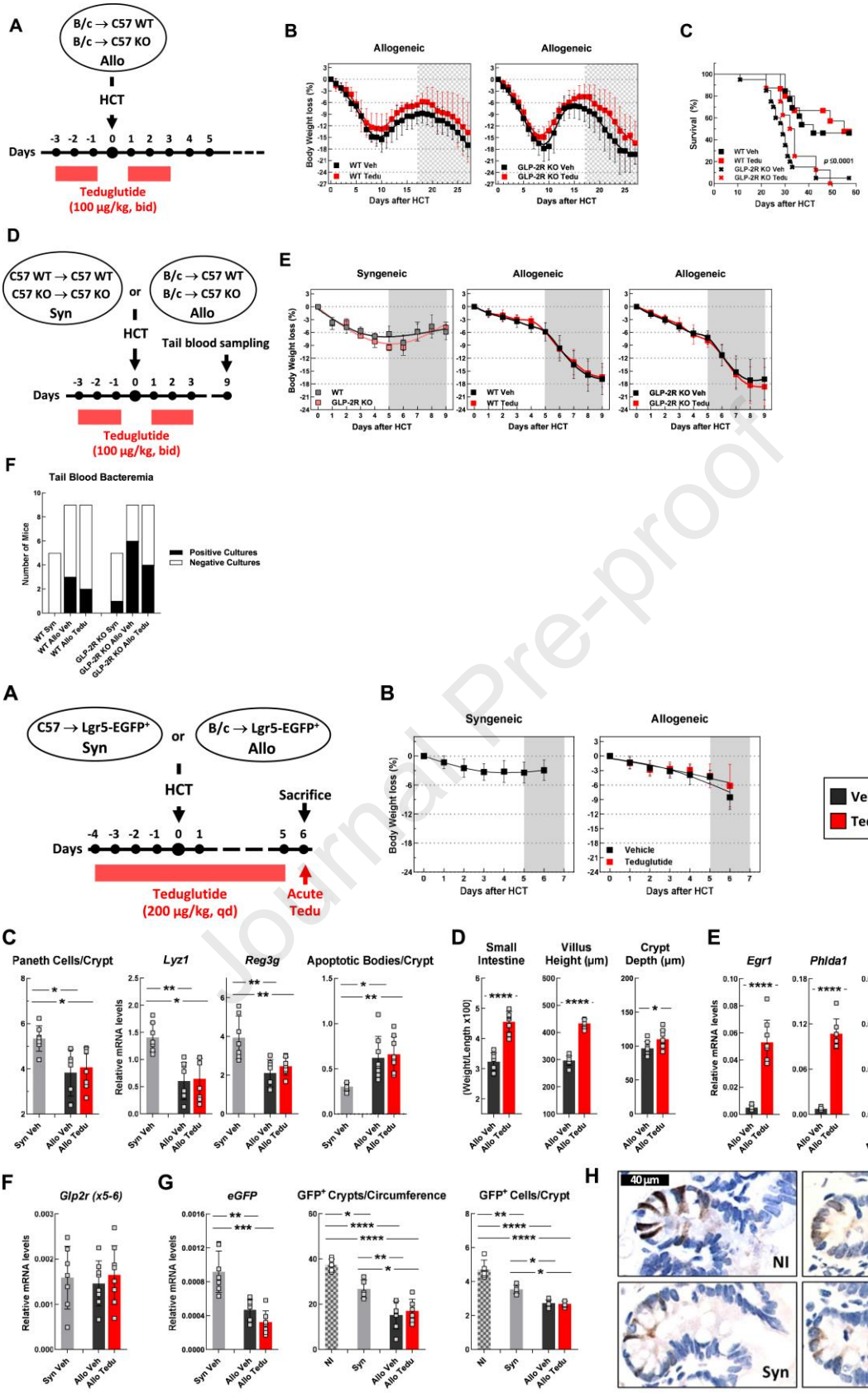
A
B/c → C57 WT
B/c → C57 KO
Allo
HCT
Days
-3 -2 -1 0 1 2 3 4 5
Teduglutide
(100 µg/kg, bid)
B
Allogeneic
Allogeneic
Body Weight loss (%)
WT Veh
WT Tedu
GLP-2R KO Veh
GLP-2R KO Tedu
Days after HCT
C
Survival (%)
WT Veh
WT Tedu
GLP-2R KO Veh
GLP-2R KO Tedu
p ≤0.0001
Days after HCT
D
C57 WT → C57 WT
C57 KO → C57 KO
Syn
or
B/c → C57 WT
B/c → C57 KO
Allo
HCT
Tail blood sampling
Days
-3 -2 -1 0 1 2 3 9
Teduglutide
(100 µg/kg, bid)
E
Syngeneic
Allogeneic
Allogeneic
Body Weight loss (%)
WT
GLP-2R KO
WT Veh
WT Tedu
GLP-2R KO Veh
GLP-2R KO Tedu
Days after HCT
F
Tail Blood Bacteremia
Number of Mice
Positive Cultures
Negative Cultures
WT Syn
WT Allo Veh
WT Allo Tedu
GLP-2R KO Syn
GLP-2R KO Allo Veh
GLP-2R KO Allo Tedu

A
C57 → Lgr5-EGFP+
Syn
or
B/c → Lgr5-EGFP+
Allo
HCT
Sacrifice
Days
-4 -3 -2 -1 0 1 5 6
Teduglutide
(200 µg/kg, qd)
Acute
Tedu
B
Syngeneic
Allogeneic
Body Weight loss (%)
Vehicle
Teduglutide
Days after HCT
Vehicle
Teduglutide
C
Paneth Cells/Crypt
Lyz1
Reg3g
Apoptotic Bodies/Crypt
Relative mRNA levels
Syn Veh
Allo Veh
Allo Tedu
D
Small Intestine (Weight/Length x100)
Villus Height (µm)
Crypt Depth (µm)
E
Egr1
Phlda1
Areg
Ereg
Relative mRNA levels
F
Glp2r (x5-6)
Relative mRNA levels
G
eGFP
GFP+ Crypts/Circumference
GFP+ Cells/Crypt
NI
Syn
H
40 µm
NI
Allo Veh
Syn
Allo Tedu

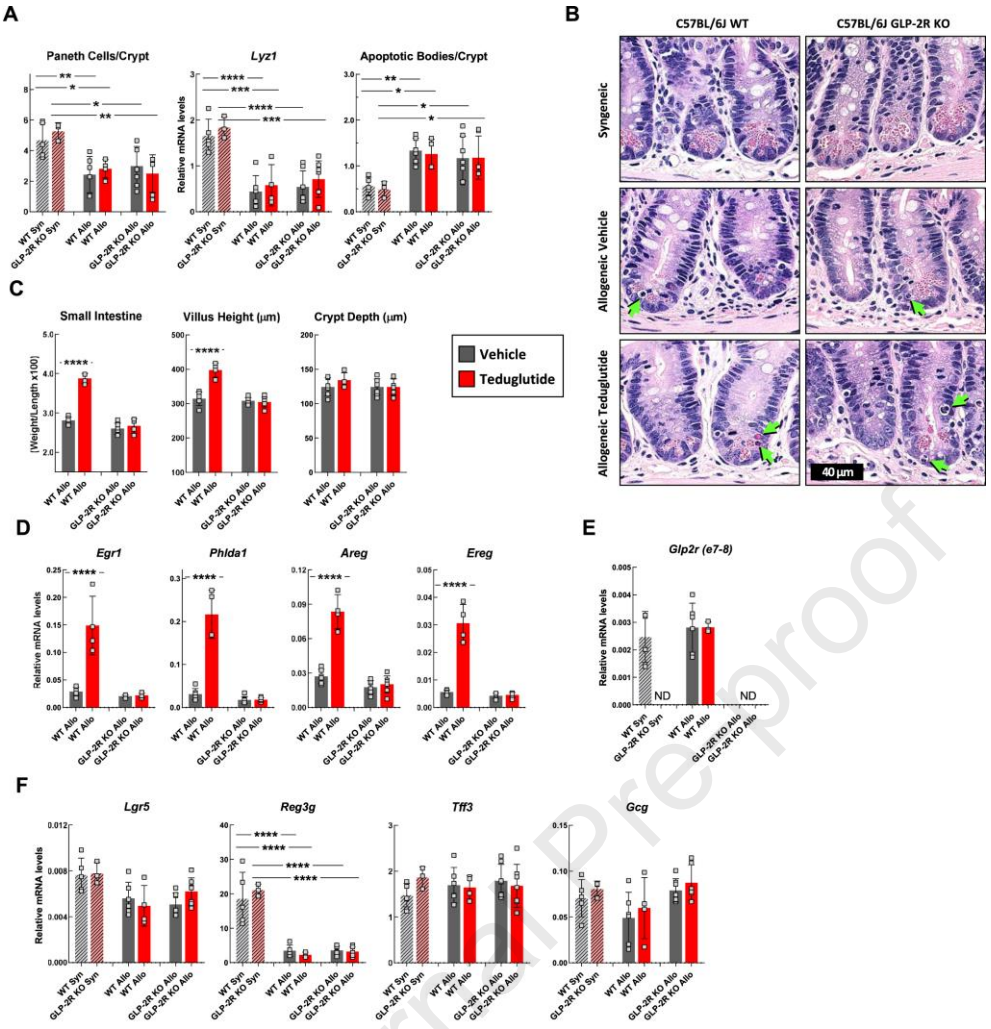

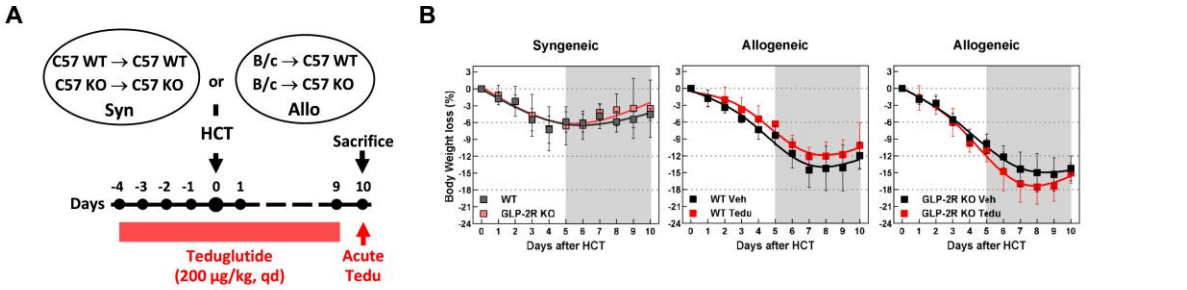
A
C57 WT → C57 WT
C57 KO → C57 KO
Syn
or
B/c → C57 WT
B/c → C57 KO
Allo
HCT
Sacrifice
-4 -3 -2 -1 0 1 9 10
Days
Teduglutide
(200 µg/kg, qd)
Acute
Tedu
B
Syngeneic
Allogeneic
Allogeneic
Body Weight loss (%)
WT
GLP-2R KO
WT Veh
WT Tedu
GLP-2R KO Veh
GLP-2R KO Tedu
Days after HCT

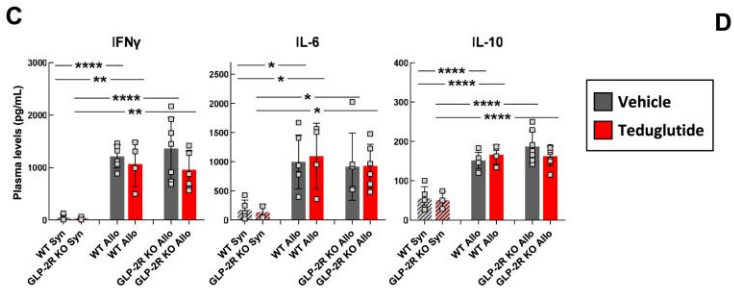
C
IFNγ
IL-6
IL-10
Plasma levels (pg/mL)
WT Syn
GLP-2R KO Syn
WT Allo
GLP-2R KO Allo
Vehicle
Teduglutide

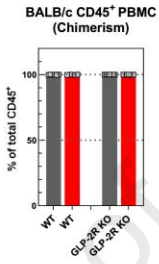
D
BALB/c CD45+ PBMC
(Chimerism)
% of total CD45+
WT
GLP-2R KO

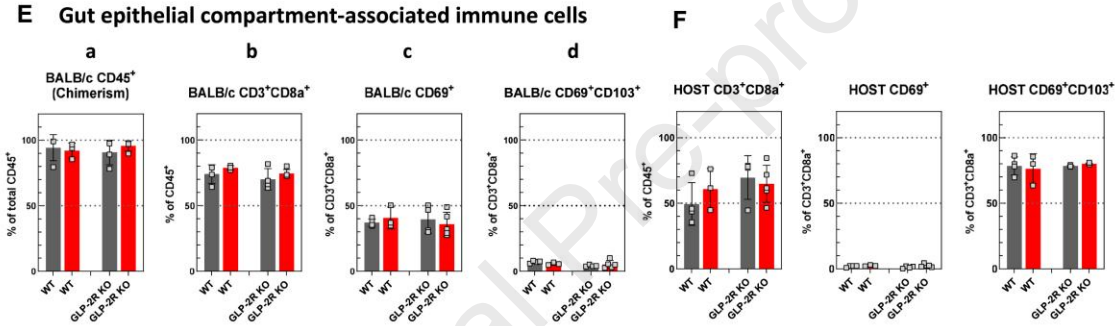
E Gut epithelial compartment-associated immune cells
a
b
c
d
BALB/c CD45+
(Chimerism)
BALB/c CD3+CD8a+
BALB/c CD69+
BALB/c CD69+CD103+
% of total CD45+
% of CD45+
% of CD3+CD8a+
WT
GLP-2R KO

F
HOST CD3+CD8a+
HOST CD69+
HOST CD69+CD103+
% of CD45+
% of CD3+CD8a+
WT
GLP-2R KO

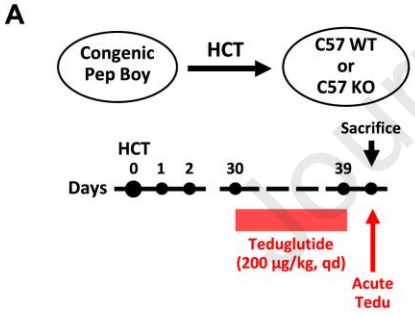
A
Congenic
Pep Boy
HCT
C57 WT
or
C57 KO
Sacrifice
HCT
0 1 2 30 39
Days
Teduglutide
(200 µg/kg, qd)
Acute
Tedu

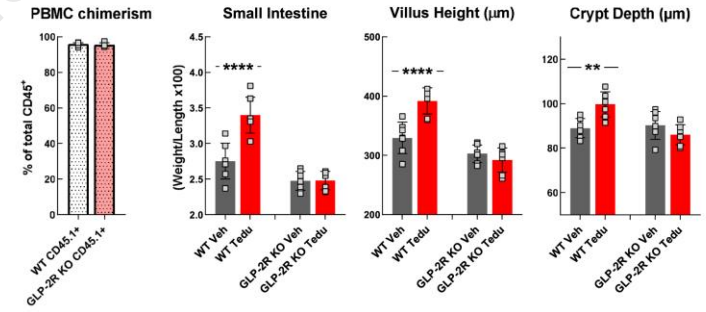
B
PBMC chimerism
% of total CD45+
WT CD45.1+
GLP-2R KO CD45.1+
C
Small Intestine
(Weight/Length x100)
Villus Height (µm)
Crypt Depth (µm)
WT Veh
WT Tedu
GLP-2R KO Veh
GLP-2R KO Tedu

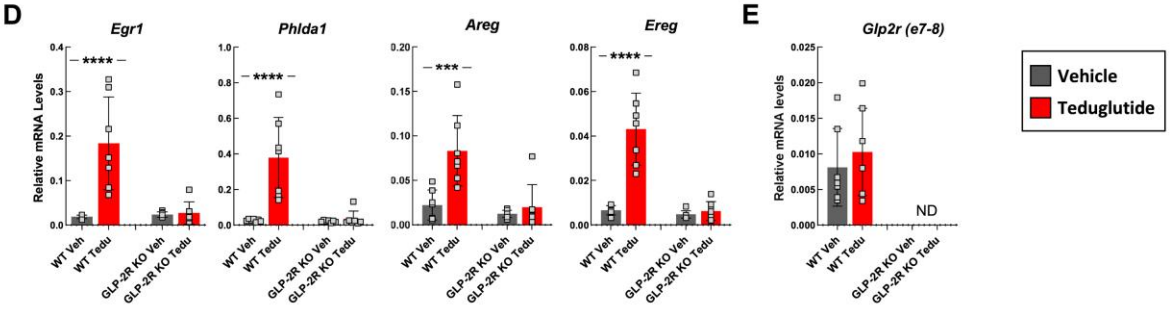
D
Egr1
Phlda1
Areg
Ereg
Relative mRNA Levels
WT Veh
WT Tedu
GLP-2R KO Veh
GLP-2R KO Tedu
E
Glp2r (e7-8)
Relative mRNA levels
ND
Vehicle
Teduglutide

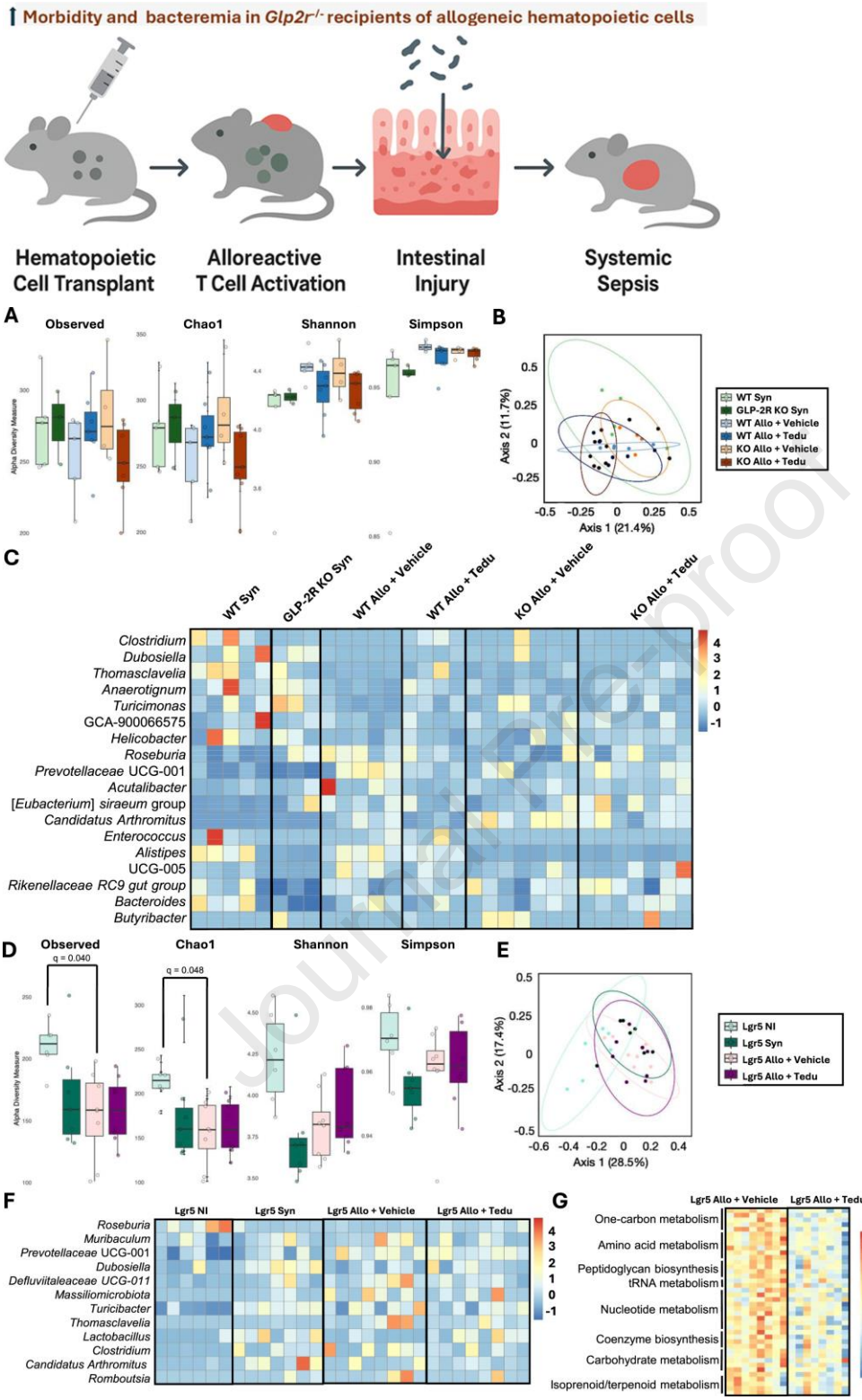
Morbidity and bacteremia in Glp2r-/- recipients of allogeneic hematopoietic cells
Hematopoietic Cell Transplant
Alloreactive T Cell Activation
Intestinal Injury
Systemic Sepsis
A
Observed
Chao1
Shannon
Simpson
Alpha Diversity Measure
B
Axis 2 (11.7%)
Axis 1 (21.4%)
WT Syn
GLP-2R KO Syn
WT Allo + Vehicle
WT Allo + Tedu
KO Allo + Vehicle
KO Allo + Tedu
C
WT Syn
GLP-2R KO Syn
WT Allo + Vehicle
WT Allo + Tedu
KO Allo + Vehicle
KO Allo + Tedu
Clostridium
Dubosiella
Thomasclavelia
Anaerotignum
Turicimonas
GCA-900066575
Helicobacter
Roseburia
Prevotellaceae UCG-001
Acutalibacter
[Eubacterium] siraeum group
Candidatus Arthromitus
Enterococcus
Alistipes
UCG-005
Rikenellaceae RC9 gut group
Bacteroides
Butyribacter
D
Observed
q = 0.040
Chao1
q = 0.048
Shannon
Simpson
Alpha Diversity Measure
E
Axis 2 (17.4%)
Axis 1 (28.5%)
Lgr5 NI
Lgr5 Syn
Lgr5 Allo + Vehicle
Lgr5 Allo + Tedu
F
Lgr5 NI
Lgr5 Syn
Lgr5 Allo + Vehicle
Lgr5 Allo + Tedu
Roseburia
Muribaculum
Prevotellaceae UCG-001
Dubosiella
Defluviitaleaceae UCG-011
Massiliomicrobiota
Turicibacter
Thomasclavelia
Lactobacillus
Clostridium
Candidatus Arthromitus
Romboutsia
G
Lgr5 Allo + Vehicle
Lgr5 Allo + Tedu
One-carbon metabolism
Amino acid metabolism
Peptidoglycan biosynthesis
tRNA metabolism
Nucleotide metabolism
Coenzyme biosynthesis
Carbohydrate metabolism
Isoprenoid/terpenoid metabolism